miR-375 affects the hedgehog signaling pathway by downregulating RAC1 to inhibit hepatic stellate cell viability and epithelial-mesenchymal transition

ZHIWEI LIANG, JIAN LI, LONGSHUAN ZHAO and YILEI DENG

Department of Hepatopancreatobiliary Surgery, The First Affiliated Hospital of Zhengzhou University, Zhengzhou, Henan 450000, P.R. China

Received May 13, 2020; Accepted October 13, 2020

DOI: 10.3892/mmr.2020.11821

Abstract. MicroRNAs (miRNAs/miRs) are a class of non-coding RNAs that serve crucial roles in liver cancer and other liver injury diseases. However, the expression profile and mechanisms underlying miRNAs in liver fibrosis are not completely understood. The present study identified the novel miR-375/Rac family small GTPase 1 (RAC1) regulatory axis in liver fibrosis. Reverse transcription-quantitative PCR was performed to detect miR-375 expression levels. MTT, flow cytometry and western blotting were performed to explore the *in vitro* roles of miR-375. The dual-luciferase reporter gene assay was performed to determine the potential mechanism underlying miR-375 in liver fibrosis. miR-375 expression was significantly downregulated in liver fibrosis tissues and cells compared with healthy control tissues and hepatocytes, respectively. Compared with the pre-negative control group, miR-375 overexpression inhibited mouse hepatic stellate cell (HSC) viability and epithelial-mesenchymal transition, and alleviated liver fibrosis. The dual-luciferase reporter assay results demonstrated that miR-375 bound to RAC1. Moreover, the results indicated that miR-375 regulated the hedgehog signaling pathway via RAC1 to restrain HSC viability and EMT, thus exerting its anti-liver fibrosis function. The present study identified the miR-375/RAC1 axis as a novel regulatory axis associated with the development of liver fibrosis.

Introduction

Liver fibrosis is a common pathological alteration that occurs during the process of tissue repair after chronic liver injury, and gradually develops into cirrhosis, which eventually leads to irreversible liver injury (1,2). Emerging evidence indicates that the abnormal activation and proliferation of hepatic stellate cells (HSCs) are important factors leading to liver fibrosis (3) and that epithelial-mesenchymal transition (EMT) is associated with the abnormal activation of HSCs (4). Choi *et al* (5) reported that EMT in HSC activation is regulated via the hedgehog (Hh) signaling pathway. Therefore, inhibiting HSC excessive viability and EMT by regulating the Hh signaling axis may serve as a potential therapeutic strategy to alleviate liver fibrosis.

MicroRNAs (miRNAs/miRs) are small non-coding RNAs composed of 22-25 nucleotides that restrain the expression of target mRNAs by binding to their 3'untranslated region (UTR) (6). Yu *et al* (7) demonstrated that increasing the expression of miR-200a regulated the Hh signaling pathway by targeting the binding to GLI family zinc finger 2 (Gli2), thus restraining EMT in HSC activation to hinder the progression of liver fibrosis. The increased expression of miR-152 regulates the Hh signaling pathway by downregulating DNA methyltransferase 1, and further restrains HSC activation and EMT to exert its anti-fibrotic function (8). A study demonstrated that the abnormal expression of miR-375 has been observed in various diseases, including inflammatory bowel disease and liver cancer, suggesting that miR-375 serves important regulatory functions in various human diseases (9). Besides, Yang *et al* (10) reported that miR-375 is downregulated in a fructose-induced liver fibrosis rat model. However, the molecular mechanism underlying miR-375 in liver fibrosis is not completely understood.

Rac family small GTPase 1 (RAC1) is an important member of the Rho family of small GTPase proteins and participates in the regulatory processes of cell proliferation, differentiation and EMT (11). RAC1 overexpression in HSCs leads to abnormal activation, which in turn aggravates liver fibrosis (12). Another study demonstrated that RAC1 activation induces HSC activation and promotes HSC EMT by mediating the Hh signaling pathway, thus aggravating liver fibrosis (13). However, the mechanism underlying RAC1 in regulating HSC activation and EMT in liver fibrosis is not completely understood.

Correspondence to: Dr Yilei Deng, Department of Hepatopancreatobiliary Surgery, The First Affiliated Hospital of Zhengzhou University, 1 Jian She Road, Zhengzhou, Henan 450000, P.R. China
E-mail: dengyilei@163.com

Key words: microRNA-375, Rac family small GTPase 1, liver fibrosis, hepatic stellate cell, epithelial-mesenchymal transition

The present study aimed to investigate the expression of miR-375 in liver fibrosis tissues and cells compared with healthy control tissues and hepatocytes (HCs), respectively. Moreover, the mechanisms underlying miR-375 in liver fibrosis were investigated.

Materials and methods

Tissue samples. In the present study, 15 healthy controls and 15 patients (43.2% male patients and 56.8% female patients; age, 60.1±11.7 years) with liver cirrhosis undergoing partial liver resection or liver biopsy were recruited from the First Affiliated Hospital of Zhengzhou University (Zhengzhou, China) between March 2017 and March 2020. Liver cirrhosis was diagnosed by performing a liver biopsy, abdominal ultrasound or computed tomography scan. The exclusion criteria were as follows: i) The use of non-protective liver drugs to treat viral hepatitis or liver fibrosis; and ii) liver biochemical indicators were normal. The participants were divided into two groups: i) Healthy controls (n=15); and ii) cirrhosis (n=15). The present study was approved by the Ethics Committee of the First Affiliated Hospital of Zhengzhou University (approval no. 2020-KY-047). Written informed consent was obtained from all patients before obtaining liver tissues.

RNA isolation and reverse transcription-quantitative PCR (RT-qPCR). RT-qPCR was performed as previously described (14). Briefly, total RNA was extracted from human and mouse liver fibrosis tissues and mouse liver fibrosis cells using TRIzol® reagent (Invitrogen; Thermo Fisher Scientific, Inc.). Total RNA was reverse transcribed into cDNA using the PrimeScript One-Step RT-PCR kit (Takara Biotechnology Co., Ltd.) at 42˚C. Subsequently, qPCR was performed using an SYBR Green PCR kit (Applied Biosystems; Thermo Fisher Scientific, Inc.) and an ABI 7900HT Fast Real-Time PCR System (Applied Biosystems; Thermo Fisher Scientific, Inc.). The following thermocycling conditions were used for qPCR: 95˚C for 5 min; followed by 40 cycles of 95˚C for 15 sec and 60˚C for 20 sec. The sequences of the primers used for qPCR are presented in Table I. miRNA and mRNA expression levels were quantified using the $2^{-\Delta\Delta Cq}$ method (15) and normalized to the internal reference genes U6 and β-actin, respectively.

Establishment of liver fibrosis mouse model. A total of 12 male C57BL/6J mice (age, 8 weeks; weight, 20-22 g; Experimental Animal Center of Zhengzhou University) were used to establish a liver fibrosis mouse model. The mice were housed in a temperature (23±3˚C) and humidity (40-70%) controlled environment with 12-h light/dark cycles, and free access to food and water. Animal health and behavior were assessed every 24 h. Mice were divided into the following two groups: i) Sham (n=6); and ii) CCl_4 (n=6). Mice in the CCl_4 group were intraperitoneally injected with 7 ml/kg CCl_4 (diluted 1:9 in olive oil; Sinopharm Chemical Reagent Co., Ltd.; cat. no. XW00562352) twice a week for six weeks. Mice in the sham group were intraperitoneally injected with the same volume of olive oil twice a week for six weeks. At the end of the six weeks, mice were sacrificed and the liver tissues were isolated for subsequent experiments. The animal experimental protocol was approved by the Ethics Committee of the First Affiliated Hospital of Zhengzhou University (approval no. 2020-KY-047).

Masson and hematoxylin and eosin (H&E) staining. Mouse liver tissue samples were fixed with 10% formalin at room temperature for 48 h, embedded in paraffin and cut into 5-μm thick sections. According to the standard protocols, Masson staining was performed to assess collagen deposition and H&E staining was performed to assess the degree of liver injury. For Masson staining, sections were stained with hematoxylin for 5-10 min at room temperature, followed by Masson staining for 5-10 min at room temperature. For H&E staining, sections were stained with hematoxylin for 5-10 min at room temperature, followed by eosin staining for 1 min at room temperature. Stained sections were observed using a light microscope (Nikon Corporation; magnification, x200).

Western blotting. Total protein was extracted from human and mouse liver fibrosis tissues and mouse liver fibrosis cells using RIPA (Beijing Solarbio Science & Technology Co., Ltd.). Total protein was quantified using the BCA Protein Assay kit (Beijing Solarbio Science & Technology Co., Ltd.). Proteins (20 μg/lane) were separated via 10% SDS-PAGE and transferred onto PVDF membranes. After blocking with 5% skim milk at room temperature for 1 h, the membranes were incubated overnight at 4˚C with the following primary antibodies: Anti-α-smooth muscle actin (α-SMA; cat. no. ab5694; 1:1,000; Abcam), anti-collagen type I-α1 (Col1A1; cat. no. ab34710; 1:1,000; Abcam), anti-RAC1 (cat. no. ab155938; 1:1,000; Abcam), anti-E-cadherin (cat. no. ab227639; 1:25; Abcam), anti-Snail (cat. no. ab216347; 1:1,000; Abcam), anti-Vimentin (cat. no. sc-6260; 1:1,000; Santa Cruz Biotechnology, Inc.), anti-hedgehog interacting protein (Hhip; cat. no. ab86450; 1:1,000; Abcam), anti-sonic hedgehog signaling molecule (Shh; cat. no. sc-365112; 1:1,000; Santa Cruz Biotechnology, Inc.), anti-Gli2 (cat. no. sc-271786; 1:1,000; Santa Cruz Biotechnology, Inc.) and anti-β-actin (cat. no. sc-8432; 1:1,000; Santa Cruz Biotechnology, Inc.). Subsequently, the membranes were incubated with a HRP-conjugated specific secondary antibody (cat. no. ab205718; 1:2,000; Abcam) at room temperature for 1 h. Protein bands were visualized using the enhanced chemiluminescence kit (Shanghai XP Biomed Ltd.). β-actin was used as the loading control.

Cell isolation and culture. Mouse primary HCs and primary HSCs were isolated as previously described (16). Cells were cultured in DMEM (Gibco; Thermo Fisher Scientific, Inc.) supplemented with 10% FBS (Gibco; Thermo Fisher Scientific, Inc.), 100 U/ml penicillin and 100 μg/ml streptomycin at 37˚C with 5% CO_2. Moreover, HSCs were isolated from healthy control mice and cultured in DMEM at 37˚C, 5% CO_2 *in vitro* for 1, 3 and 5 days, respectively.

Cell transfection and treatment. HSCs were isolated from healthy control mice (Sham group) and cultured for 1 day *in vitro* to obtain primary-1-day HSCs. Primary-1-Day HSCs were seeded ($1x10^5$ cells/well) into 24-well plates and cultured for ~24 h. At 80% confluence, cells were transfected with 10 nM miR-375 mimic, 10 nM pre-NC, 10 nM miR-375 mimic + 10 nM pcDNA-RAC1, 10 nM miR-375 inhibitor or 10 nM NC at 37˚C for

Table I. Sequences of primers used for reverse transcription-quantitative PCR.

Gene	Sequence (5'→3')
miR-375	F: CACAAAATTTGTTCGTTCGGCT
	R: GTGCAGGGTCCGAGGT
U6	F: CAAATTCGTGAAGCGTTCCATAT
	R: GCTTCACGAATTTGCGTGTCATCCTTGC
RAC1	F: GAGCAGAAGCTGATCTCCGAGGAG
	R: TTACAACAGCAGGCATTTTCTCTT
α-SMA	F: CTGACAGAGGCACCACTGAA
	R: CATCTCCAGAGTCCAGCACA
Col1A1	F: GATTGAGAACATCCGCAGC
	R: CATCTTGAGGTCACGGCAT
β-actin	F: CAGGAGGCATTGCTGATGAT
	R: GAAGGCTGGGGCTCATTT

miR, microRNA; RAC1, Rac family small GTPase 1; α-SMA, α-smooth muscle actin; Col1A1, collagen type I-α1; F, forward; R, reverse.

48 h using Lipofectamine® 2000 transfection reagent (Invitrogen; Thermo Fisher Scientific, Inc.) according to the manufacturer's protocol. miR-375 mimic, miR-375 inhibitor, pre-NC, inhibitor NC, pcDNA and pcDNA-RAC1 were purchased from Shanghai GenePharma Co., Ltd. The specific sequences were as follows: miR-375 mimic, 5'-UUUGUUCGUUCGGCUCGCGUGA-3'; miR-375 inhibitor, 5'-UCACGCGAGCCGAACGAACAAA-3'; pre-NC, 5'-CAGUACUUUUGUGUAGUACAA-3'; and NC, 5'-CAGUACUUUUGUGUAGUACAA-3'. At 48 h post-transfection, cells were used for subsequent experiments.

To investigate whether miR-375 inhibited mouse HSC viability and EMT via the Hh signaling pathway, cells ($1x10^5$) were cultured in DMEM supplemented with 0.3 μM smoothened agonist (SAG; an exogenous Hh agonist; Beyotime Institute of Biotechnology) at 37˚C for 24 h.

Cell viability. The MTT assay was performed to assess mouse HSC viability. HSC cells were seeded ($1x10^4$ cells/well) into 96-well plates and cultured at 37˚C for 48 h. Subsequently, 20 μl MTT solution was added to each well and incubated at 37˚C for 2 h. Then, 150 μl DMSO was added to dissolve the purple formazan crystals. The optical density was measured at a wavelength of 570 nm to determine HSC viability.

Cell cycle assay. The cell cycle distribution of mouse HSCs was assessed via flow cytometry. Following fixation with 70% ethanol for at 37˚C for 24 h, cells ($1x10^6$) were resuspended in PI/RNase staining buffer (BD Pharmingen; BD Biosciences) supplemented with 50 ng/μl RNase A and incubated at 37˚C for 30 min. The cell cycle distribution was analyzed via flow cytometry using an Attune™ NxT Flow Cytometer flow cytometer (Invitrogen; Thermo Fisher Scientific, Inc.) and FlowJo software (version 10; Flow Jo LLC).

Dual-luciferase reporter gene assay. Online bioinformatics software TargetScan (version 3.1; www.targetscan.org/mamm_31) was used to predict that miR-375 contained the binding sites in the 3'UTR region of RAC1.

The RAC1 3'-UTR-wild-type (WT) and RAC1 3'UTR-mutant (Mut) sequences were inserted into the pmirGLO luciferase reporter vector (Shanghai GenePharma Co., Ltd.). Subsequently, HSCs ($1x10^6$) were co-transfected with 1 μg miR-375 mimic, pre-NC, miR-375 inhibitor or NC and 1 μg RAC1 3'UTR-WT or RAC1 3'UTR-Mut using Lipofectamine 2000 transfection reagent. At 48 h post-transfection, luciferase activity was measured using a Dual-Luciferase Reporter Assay system (Promega Corporation). Firefly luciferase activity was normalized to *Renilla* luciferase activity.

Statistical analysis. Experiments were repeated at least three times. Statistical analyses were performed using SPSS software (version 17.0; SPSS, Inc.). Comparisons between two groups were analyzed using the unpaired Student's t-test. Comparisons among multiple groups were analyzed using one-way ANOVA followed by Tukey's post hoc test. $P<0.05$ was considered to indicate a statistically significant difference.

Results

miR-375 is downregulated in liver fibrosis tissues and cells. The abnormal expression of miRNAs is associated with the occurrence of liver fibrosis (17,18). In the present study, the expression levels of miR-375 and Col1A1 (a liver fibrosis molecular marker) in the tissue samples of patients with cirrhosis were assessed. Compared with the healthy control group, miR-375 expression was significantly decreased in the cirrhosis group, whereas Col1A1 expression was significantly increased (Fig. 1A). Pearson's correlation analysis demonstrated that miR-375 expression was negatively correlated with Col1A1 expression and RAC1 expression in human cirrhosis tissue samples (Fig. 1B). Subsequently, a liver fibrosis mouse model was established via intraperitoneal injection of CCl_4. The Masson and H&E staining results indicated that the liver fibrosis tissues of mice in the CCl_4 group displayed increased collagen deposition, inflammation, infiltration, steatosis and fibrosis compared with the sham group (Fig. 1C). α-SMA and Col1A1 are common molecular marker of liver fibrosis (19). The mRNA and protein expression levels of α-SMA and Col1A1 were dramatically increased in the CCl_4 group compared with the sham group (Fig. 1D). By contrast, miR-375 expression was significantly decreased in the CCl_4 group compared with the sham group (Fig. 1E). Subsequently, mouse primary HCs and primary HSCs were isolated from liver fibrosis model mice. miR-375 expression was significantly decreased in the HSC group compared with the HC group (Fig. 1F). Moreover, HSCs were isolated from healthy control mice and cultured *in vitro* for 1, 3 and 5 days, respectively. The mRNA and protein expression levels of α-SMA and Col1A1 were markedly increased in the day 3 and 5 groups compared with the day 1 group (Fig. 1G). By contrast, miR-375 expression was significantly decreased in the day 3 and 5 groups compared with the day 1 group (Fig. 1H). The aforementioned results indicated that miR-375 was downregulated in human and mouse liver fibrosis tissues and mouse liver fibrosis cells compared with healthy control tissues and HCs, respectively, suggesting that miR-375 may serve a regulatory function in the process of liver fibrosis.

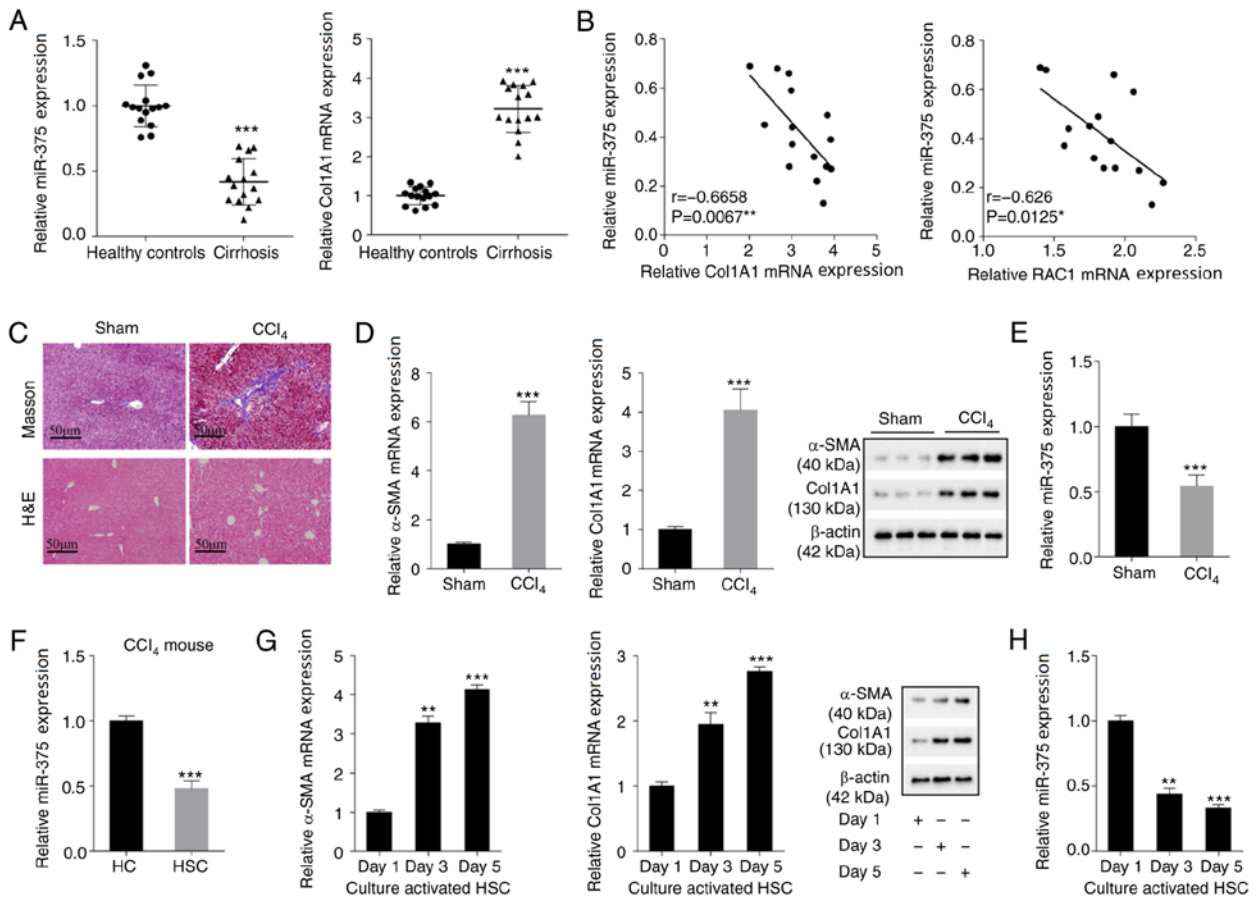

Figure 1. miR-375 expression in liver fibrosis tissues and cells. Liver tissues were isolated from healthy controls (n=15) and patients with cirrhosis (n=15) who underwent partial liver resection or liver biopsy. (A) miR-375 and Col1A1 (a liver fibrosis molecular marker) expression levels in the tissue samples of healthy controls and patients with cirrhosis. (B) Pearson's correlation analysis was performed to analyze the correlation between miR-375 expression and Col1A1 or RAC1 expression in tissue samples isolated from patients with cirrhosis. A liver fibrosis mouse model of liver fibrosis was established by an intraperitoneal injection of CCl_4. (C) Pathological alterations in tissue samples isolated from liver fibrosis mouse models were observed by performing Masson and H&E staining (scale bar, 50 μm). (D) α-SMA and Col1A1 mRNA and protein expression levels in the liver fibrosis mouse model. (E) miR-375 expression in the liver fibrosis mouse model. Primary HCs and HSCs were isolated from liver fibrosis model mice. (F) miR-375 expression in primary HCs and HSCs. HSCs isolated from healthy control mice were cultured *in vitro* for 1, 3 and 5 days. (G) α-SMA and Col1A1 mRNA and protein expression levels in HSCs. (H) miR-375 expression in HSCs. *P<0.05, **P<0.01 and ***P<0.001 vs. healthy control, Sham, HC or day 1. miR, microRNA; Col1A1, collagen type I-α1; RAC1, Rac family small GTPase 1; H&E, hematoxylin and eosin; α-SMA, α-smooth muscle actin; HC, hepatocyte; HSC, hepatic stellate cell.

miR-375 overexpression inhibits mouse HSC viability and EMT, and alleviates liver fibrosis. To further investigate the function of miR-375 in liver fibrosis, HSCs isolated from healthy control mice were cultured for 1 day *in vitro* to obtain mouse primary-1-day HSC. Subsequently, primary-1-day HSCs were transfected with miR-375 mimic or pre-NC. miR-375 mimic significantly increased miR-375 expression compared with pre-NC (Fig. 2A), indicating successful overexpression of miR-375 in mouse primary-1-day HSC. miR-375 overexpression notably decreased the mRNA and protein expression levels of α-SMA, Col1A1 and RAC1 compared with the pre-NC group (Fig. 2B). Moreover, the MTT assay results indicated that miR-375 overexpression significantly inhibited HSC viability compared with the pre-NC group (Fig. 2C). The cell cycle analysis results suggested that miR-375 overexpression significantly inhibited the cell cycle progression of HSCs compared with the pre-NC group (Figs. 2D and S1A). The western blotting results indicated that compared with the pre-NC group, miR-375 mimic markedly increased the protein expression levels of the epithelial marker E-cadherin and the Hh signaling pathway-related molecule Hhip. However, compared with the pre-NC group, miR-375 mimic notably decreased the protein expression levels of the mesenchymal markers Snail and Vimentin, and the Hh signaling pathway-related molecules Shh and Gli2 (Fig. 2E). The aforementioned results indicated that miR-375 overexpression inhibited mouse HSC viability and EMT, and alleviated liver fibrosis.

miR-375 inhibits mouse HSC viability and EMT via the Hh signaling pathway. miR-375-mediated effects on mouse HSC viability and EMT were further investigated. Primary-1-day HSCs were transfected with miR-375 mimic and at 48 h post-transfection, cells were cultured in DMEM supplemented with 0.3 μM SAG (an exogenous Hh agonist) for 24 h. Compared with pre-NC, miR-375 overexpression markedly decreased the mRNA and protein expression levels of α-SMA and Col1A1, which was reversed by treatment with SAG (Fig. 3A). Moreover, the western blotting results indicated that miR-375 overexpression notably increased the protein expression levels of E-cadherin and Hhip, but decreased the expression levels of Snail, Vimentin, Shh and Gli2 compared with the pre-NC group. miR-375 overexpression-mediated effects on protein expression were markedly reversed by treatment with SAG (Fig. 3B). The MTT assay results

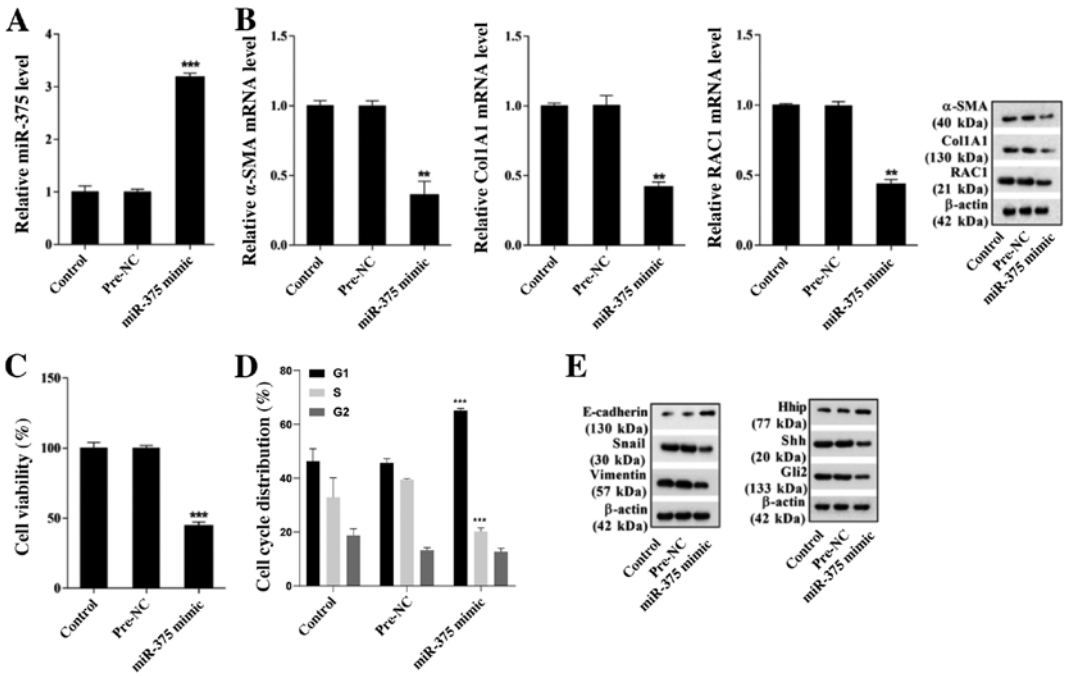

Figure 2. Effect of miR-375 on mouse HSC viability, EMT and liver fibrosis. HSCs were isolated from healthy control mice and cultured *in vitro* for 1 day to obtain primary-1-day HSCs. Primary-1-day HSCs were transfected with miR-375 mimic or pre-NC. (A) miR-375 expression. (B) α-SMA, Col1A1 and RAC1 mRNA and protein expression levels. (C) The MTT assay was performed to assess HSC viability. (D) Flow cytometry was performed to assess the cell cycle distribution in HSCs. (E) The protein expression levels of epithelial marker E-cadherin, mesenchymal markers Snail and Vimentin, and hedgehog signaling pathway-related molecules Hhip, Shh and Gli2. **P<0.01 and ***P<0.001 vs. pre-NC. miR, microRNA; HSC, hepatic stellate cell; EMT, epithelial-mesenchymal transition; NC, negative control; α-SMA, α-smooth muscle actin; Col1A1, collagen type I-α1; RAC1, Rac family small GTPase 1; Snail, snail family transcriptional repressor 1; Hhip, hedgehog interacting protein; Shh, sonic hedgehog signaling molecule; Gli2, GLI family zinc finger 2.

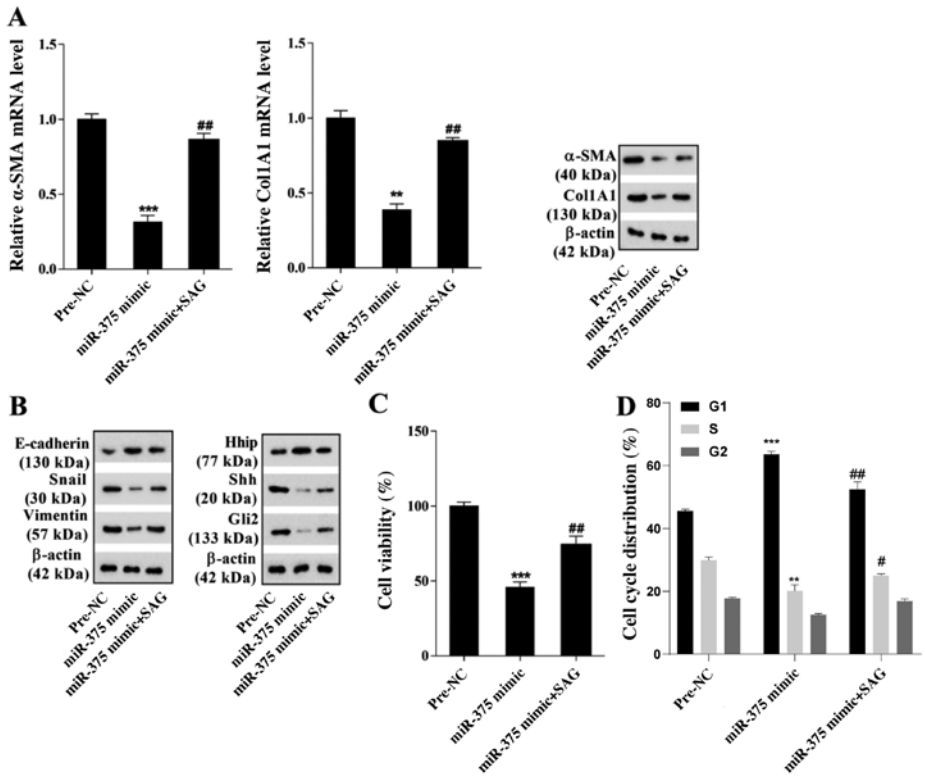

Figure 3. miR-375 affects mouse HSC viability and EMT via the Hh signaling pathway. Primary-1-day HSCs were transfected with miR-375 mimic and at 48 h post-transfection, cells were cultured in DMEM supplemented with 0.3 μM SAG (an exogenous Hh agonist) for 24 h. (A) α-SMA and Col1A1 mRNA and protein expression levels. (B) E-cadherin, Snail, Vimentin, Hhip, Shh and Gli2 protein expression levels. (C) The MTT assay was performed to assess HSC viability. (D) Flow cytometry was performed to assess the cell cycle distribution in HSCs. **P<0.01 and ***P<0.001 vs. pre-NC; $^{\#}$P<0.05 and $^{\#\#}$P<0.01 vs. miR-375 mimic. miR, microRNA; HSC, hepatic stellate cell; EMT, epithelial-mesenchymal transition; Hh, hedgehog; SAG, smoothened agonist; α-SMA, α-smooth muscle actin; Col1A1, collagen type I-α1; Snail, snail family transcriptional repressor 1; Hhip, hedgehog interacting protein; Shh, sonic hedgehog signaling molecule; Gli2, GLI family zinc finger 2; NC, negative control.

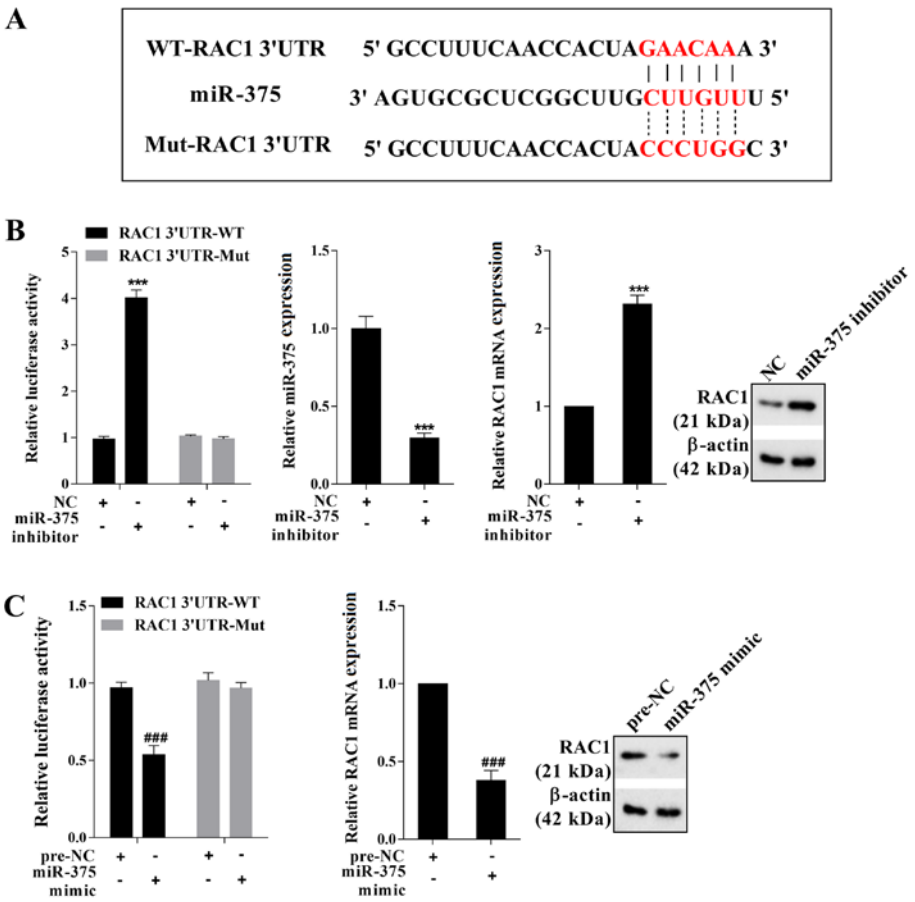

Figure 4. miR-375-mediated regulation of RAC1 expression. (A) TargetScan was used to identify the binding sites between miR-375 and RAC1. A dual-luciferase reporter gene assay was performed to assess the effects of (B) miR-375 inhibitor and (C) miR-375 mimic on the luciferase activity of RAC1 and RAC1 expression. ***P<0.001 vs. NC; ###P<0.001 vs. pre-NC. miR, microRNA; RAC1, Rac family small GTPase 1; NC, negative control; WT, wild-type; Mut, mutant; UTR, untranslated region.

demonstrated that compared with the pre-NC group, miR-375 overexpression significantly inhibited mouse HSC viability, which was significantly reversed by treatment with SAG (Fig. 3C). The cell cycle analysis results demonstrated that compared with the pre-NC group, miR-375 overexpression significantly inhibited cell cycle progression in mouse HSCs, which was also significantly reversed by treatment with SAG (Figs. 3D and S1B). The results further indicated that miR-375 inhibited mouse HSC viability and EMT via the Hh signaling pathway.

miR-375 negatively regulates RAC1 expression. To determine the mechanism underlying miR-375-mediated regulation of HSC viability and EMT in mice, the online bioinformatics software TargetScan was used. The results indicated that RAC1 was a potential target gene of miR-375 (Fig. 4A). The transfection efficiency of miR-375 inhibitor was presented in Fig. 4B. The dual-luciferase reporter gene assay results indicated that miR-375 negatively regulated the luciferase activity of RAC1 3'UTR-WT (Fig. 4B and C). Moreover, miR-375 negatively regulated the mRNA and protein expression levels of RAC1 (Fig. 4B and C). Therefore, the aforementioned results indicated that miR-375 negatively regulated RAC1 expression by binding to the 3'UTR of RAC1.

miR-375 inhibits mouse HSC viability and EMT by regulating the Hh signaling pathway via RAC1. To further assess whether miR-375 regulated mouse HSC viability and EMT via targeting RAC1, miR-375 mimic, miR-375 mimic + pcDNA-RAC1 and their corresponding controls were transfected into mouse primary-1-day HSC.

Compared with the corresponding control groups, RAC1 overexpression significantly increased RAC1 expression, indicating successful overexpression of RAC1 in mouse primary-1-day HSCs (Fig. 5A). The RT-qPCR and western blotting results indicated that compared with the pre-NC group, miR-375 overexpression markedly decreased the mRNA and protein expression levels of RAC1, α-SMA and Col1A1, which was reversed by co-transfection with pcDNA-RAC1 (Fig. 5B-D). Moreover, compared with the pre-NC group, miR-375 overexpression notably increased the protein expression levels of E-cadherin and Hhip, and decreased the protein expression levels of Snail, Vimentin, Shh and Gli2. miR-375 overexpression-mediated effects on protein expression were reversed by co-transfection with pcDNA-RAC1 (Fig. 5D and E). Furthermore, compared with the pre-NC group, miR-375 overexpression significantly inhibited mouse HSC viability, which was significantly reversed by co-transfection with pcDNA-RAC1 (Fig. 5F). The cell cycle analysis results suggested that compared with the pre-NC group, miR-375 overexpression significantly restrained cell cycle progression in mouse HSCs, which was reversed by co-transfection with pcDNA-RAC1 (Figs. 5G and S1C). The

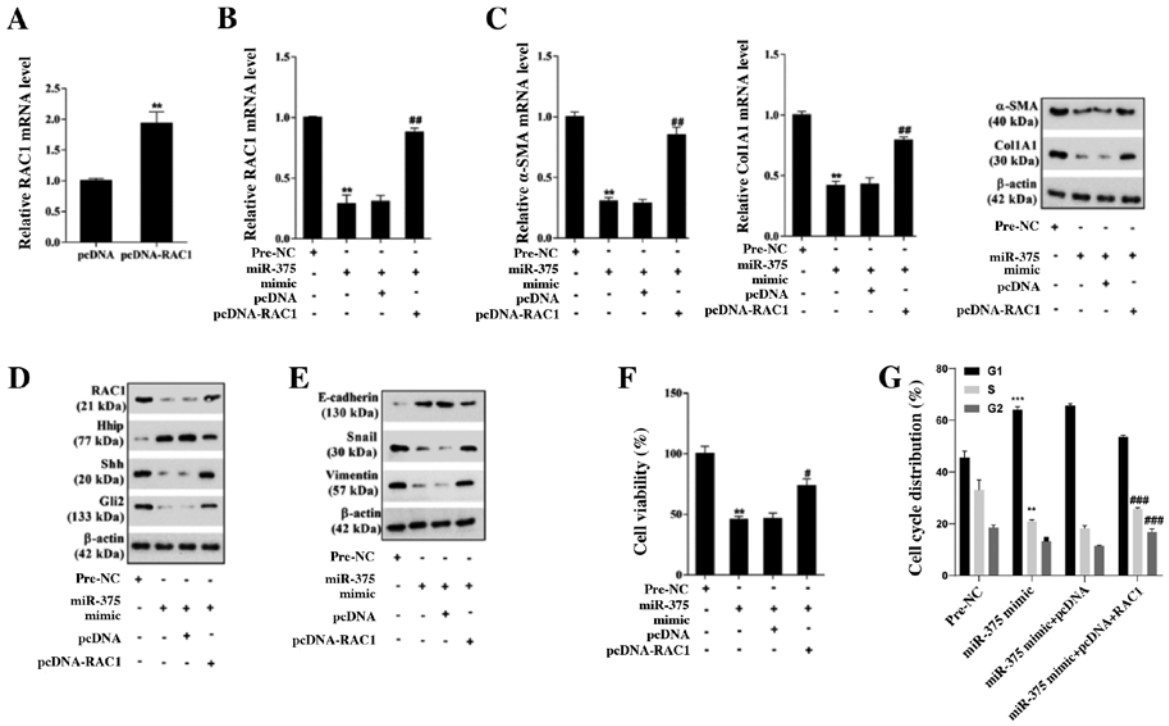

Figure 5. miR-375 affects mouse HSC viability and EMT by regulating the hedgehog signaling pathway via RAC1. Primary-1-day HSCs were transfected with miR-375 mimic, miR-375 mimic + pcDNA-RAC1 or their corresponding controls. Transfection efficiency of (A) pcDNA-RAC1. (B) RAC1 mRNA expression levels. (C) α-SMA and Col1A1 mRNA and protein expression levels. (D) RAC1, Hhip, Shh, Gli2, (E) E-cadherin, Snail and Vimentin protein expression levels. (F) The MTT assay was performed to assess HSC viability. (G) Flow cytometry was performed to assess the cell cycle distribution in HSCs. **P<0.01 and ***P<0.001 vs. pcDNA or pre-NC; $^{\#}$P<0.05, $^{\#\#}$P<0.01 and $^{\#\#\#}$P<0.001 vs. miR-375 mimic + pcDNA. miR, microRNA; HSC, hepatic stellate cell; EMT, epithelial-mesenchymal transition; RAC1, Rac family small GTPase 1; α-SMA, α-smooth muscle actin; Col1A1, collagen type I-α1; Hhip, hedgehog interacting protein; Shh, sonic hedgehog signaling molecule; Gli2, GLI family zinc finger 2; Snail, snail family transcriptional repressor 1; NC, negative control.

results indicated that miR-375 inhibited mouse HSC viability and EMT by regulating the Hh signaling pathway via RAC1.

Discussion

A previous study explored the potential mechanism underlying miRNAs in liver fibrosis (20). The present study demonstrated that miR-375 expression was significantly downregulated in liver fibrosis tissues and cells compared with healthy control tissues and HCs, respectively. Moreover, the results suggested that miR-375 interacted with RAC1. The further mechanistic studies indicated that miR-375 regulated the Hh signaling pathway via RAC1 to inhibit HSC viability and EMT, thus inhibiting liver fibrosis.

A previous study indicated that miRNAs bind to the 3'UTR of their target mRNAs to negatively regulate the expression of the target mRNA, thus serving key regulatory functions in the occurrence and development of liver fibrosis (21). For example, miR-146a is downregulated in liver fibrosis tissues, and miR-146a overexpression reduces hepatic EMT by targeting SMAD4, thus inhibiting the progression of liver fibrosis (22). Moreover, miR-375 has been reported to be downregulated in the liver fibrosis rat model (10). However, the function of miR-375 in liver fibrosis is not completely understood. The present study demonstrated that miR-375 expression was significantly downregulated in mouse liver fibrosis tissues and cells compared with sham tissues and HCs, respectively. Moreover, compared with the pre-NC group, miR-375 overexpression inhibited mouse HSC viability and EMT via the Hh signaling pathway, thus alleviating liver injury in liver fibrosis model mice.

RAC1, an important member of the Rho family of small GTPase proteins, is associated with the occurrence and development of various human diseases, including Alzheimer's disease (23,24). A previous study reported that RAC1 knockdown inhibits the development of liver fibrosis in mice (25). Choi *et al* reported that RAC1 activation induces HSC activation and promotes HSC EMT by mediating the Hh signaling pathway, thus improving liver fibrosis) and suggesting that RAC1 is involved in the development of liver fibrosis. Moreover, Venugopal *et al* demonstrated that RAC1 expression is negatively regulated by miR-194 and serves a role in liver fibrosis by regulating HSC activation (26). The present study identified binding sites between RAC1 and miR-375 using TargetScan online bioinformatics prediction software. Moreover, the results indicated that RAC1 expression was negatively regulated by miR-375. Further in-depth studies suggested that miR-375 affected the Hh signaling pathway by downregulating RAC1 to restrain HSC viability and EMT.

To conclude, the present study demonstrated that miR-375 expression was significantly downregulated in liver fibrosis tissues and cells compared with healthy control tissues and HCs, respectively. The results indicated that miR-375 regulated the Hh signaling pathway via RAC1 to inhibit HSC viability and EMT, thus relieving liver fibrosis. The results of the present study suggested that the miR-375/RAC1 axis may serve as a novel therapeutic target for liver fibrosis.

Acknowledgements

Not applicable.

Funding

No funding was received.

Availability of data and materials

The datasets used and/or analyzed during the current study are available from the corresponding author on reasonable request.

Authors' contributions

ZL designed the study, wrote the manuscript and performed the experiments. JL participated in performing the experiments and writing the manuscript. LZ acquired, analyzed and interpreted the data. YD substantially contributed to the conception and design of the study, and critically revised the manuscript. All authors read and approved the final manuscript.

Ethics approval and consent to participate

The present study was approved by the Ethics Committee of the First Affiliated Hospital of Zhengzhou University (approval no. 2020-KY-047). Written informed consent was obtained from all patients before obtaining liver tissues.

Patient consent for publication

Not applicable.

Competing interests

The authors declare that they have no competing interests.

References

1. Breitkopf-Heinlein K, Meyer C, König C, Gaitantzi H, Addante A, Thomas M, Wiercinska E, Cai C, Li Q, Wan F, *et al*: BMP-9 interferes with liver regeneration and promotes liver fibrosis. Gut 66: 939-954, 2017.
2. Hernandez-Gea V and Friedman SL: Pathogenesis of liver fibrosis. Annu Rev Pathol 6: 425-456, 2011.
3. Li W, Zhou C, Fu Y, Chen T, Liu X, Zhang Z and Gong T: Targeted delivery of hyaluronic acid nanomicelles to hepatic stellate cells in hepatic fibrosis rats. Acta Pharm Sin B 10: 693-710, 2020.
4. Yu F, Geng W, Dong P, Huang Z and Zheng J: LncRNA-MEG3 inhibits activation of hepatic stellate cells through SMO protein and miR-212. Cell Death Dis 9: 1014, 2018.
5. Choi SS, Syn WK, Karaca GF, Omenetti A, Moylan CA, Witek RP, Agboola KM, Jung Y, Michelotti GA and Diehl AM: Leptin promotes the myofibroblastic phenotype in hepatic stellate cells by activating the hedgehog pathway. J Biol Chem 285: 36551-36560, 2010.
6. Bartel DP: MicroRNAs: Genomics, biogenesis, mechanism, and function. Cell 116: 281-297, 2004.
7. Yu F, Zheng Y, Hong W, Chen B, Dong P and Zheng J: MicroRNA-200a suppresses epithelial-to-mesenchymal transition in rat hepatic stellate cells via GLI family zinc finger 2. Mol Med Rep 12: 8121-8128, 2015.
8. Yu F, Lu Z, Chen B, Wu X, Dong P and Zheng J: Salvianolic acid B-induced microRNA-152 inhibits liver fibrosis by attenuating DNMT1-mediated Patched1 methylation. J Cell Mol Med 19: 2617-2632, 2015.
9. Wang C, Luo J, Chen Z, Ye M, Hong Y, Liu J, Nie J, Zhao Q and Chang Y: MiR-375 impairs the invasive capabilities of hepatoma cells by targeting HIF1α under hypoxia. Dig Dis Sci: Mar 25, 2020 (Epub ahead of print). doi: 10.1007/s10620-020-06202-9.
10. Yang YZ, Zhao XJ, Xu HJ, Wang SC, Pan Y, Wang SJ, Xu Q, Jiao RQ, Gu HM and Kong LD: Magnesium isoglycyrrhizinate ameliorates high fructose-induced liver fibrosis in rat by increasing miR-375-3p to suppress JAK2/STAT3 pathway and TGF-β1/Smad signaling. Acta Pharmacol Sin 40: 879-894, 2019.
11. Ungefroren H, Witte D and Lehnert H: The role of small GTPases of the Rho/Rac family in TGF-β-induced EMT and cell motility in cancer. Dev Dyn 247: 451-461, 2018.
12. Choi SS, Sicklick JK, Ma Q, Yang L, Huang J, Qi Y, Chen W, Li YX, Goldschmidt-Clermont PJ and Diehl AM: Sustained activation of Rac1 in hepatic stellate cells promotes liver injury and fibrosis in mice. Hepatology 44: 1267-1277, 2006.
13. Choi SS, Witek RP, Yang L, Omenetti A, Syn WK, Moylan CA, Jung Y, Karaca GF, Teaberry VS, Pereira TA, *et al*: Activation of Rac1 promotes hedgehog-mediated acquisition of the myofibroblastic phenotype in rat and human hepatic stellate cells. Hepatology 52: 278-290, 2010.
14. Ge B, Wu H, Shao D, Li S and Li F: Interfering with miR-24 alleviates rotenone-induced dopaminergic neuron injury via enhancing autophagy by up-regulating DJ-1. Aging Pathobiol Ther 1: 17-24, 2019.
15. Livak KJ and Schmittgen TD: Analysis of relative gene expression data using real-time quantitative PCR and the 2(-Delta Delta C(T)) method. Methods 25: 402-408, 2001.
16. Yu F, Chen B, Dong P and Zheng J: HOTAIR epigenetically modulates PTEN expression via MicroRNA-29b: A novel mechanism in regulation of liver fibrosis. Mol Ther 25: 205-217, 2017.
17. Zhou X, Xiong J, Lu S, Luo L, Chen ZL, Yang F, Jin F, Wang Y, Ma Q, Luo YY, *et al*: Inhibitory effect of corilagin on miR-21-regulated hepatic fibrosis signaling pathway. Am J Chin Med 47: 1541-1569, 2019.
18. Wu JC, Chen R, Luo X, Li ZH, Luo SZ and Xu MY: MicroRNA-194 inactivates hepatic stellate cells and alleviates liver fibrosis by inhibiting AKT2. World J Gastroenterol 25: 4468-4480, 2019.
19. Li BB, Li DL, Chen C, Liu BH, Xia CY, Wu HJ, Wu CQ, Ji GQ, Liu S, Ni W, *et al*: Potentials of the elevated circulating miR-185 level as a biomarker for early diagnosis of HBV-related liver fibrosis. Sci Rep 6: 34157, 2016.
20. Wei S, Wang Q, Zhou H, Qiu J, Li C, Shi C, Zhou S, Liu R and Lu L: miR-455-3p alleviates hepatic stellate cell activation and liver fibrosis by suppressing HSF1 expression. Mol Ther Nucleic Acids 16: 758-769, 2019.
21. Yang L, Dong C, Yang J, Yang L, Chang N, Qi C and Li L: MicroRNA-26b-5p inhibits mouse liver fibrogenesis and angiogenesis by targeting PDGF receptor-beta. Mol Ther Nucleic Acids 16: 206-217, 2019.
22. Zou Y, Li S, Li Z, Song D, Zhang S and Yao Q: MiR-146a attenuates liver fibrosis by inhibiting transforming growth factor-β1 mediated epithelial-mesenchymal transition in hepatocytes. Cell Signal 58: 1-8, 2019.
23. Kikuchi M, Sekiya M, Hara N, Miyashita A, Kuwano R, Ikeuchi T, Iijima KM and Nakaya A: Disruption of a RAC1-centred network is associated with Alzheimer's disease pathology and causes age-dependent neurodegeneration. Hum Mol Genet 29: 817-833, 2020.
24. Kai Y, Kon R, Ikarashi N, Chiba Y, Kamei J and Sakai H: Role of Rac1 in augmented endothelin-1-induced bronchial contraction in airway hyperresponsive mice. J Pharmacol Sci 141: 106-110, 2019.
25. Bopp A, Wartlick F, Henninger C, Kaina B and Fritz G: Rac1 modulates acute and subacute genotoxin-induced hepatic stress responses, fibrosis and liver aging. Cell Death Dis 4: e558, 2013.
26. Venugopal SK, Jiang J, Kim TH, Li Y, Wang SS, Torok NJ, Wu J and Zern MA: Liver fibrosis causes downregulation of miRNA-150 and miRNA-194 in hepatic stellate cells, and their overexpression causes decreased stellate cell activation. Am J Physiol Gastrointest Liver Physiol 298: G101-G106, 2010.